Published in final edited form as:
Neurobiol Dis. 2014 August ; 68: 16–25. doi:10.1016/j.nbd.2014.03.014.

Role of the hippocampus in $Na_v1.6$ (*Scn8a*) mediated seizure resistance

Christopher D Makinson[#1], **Brian S Tanaka**[#2], **Tyra Lamar**[1], **Alan L Goldin**[2,b], and **Andrew Escayg**[1,b]

[1]Department of Human Genetics, Emory University, Atlanta, GA 30322

[2]Departments of Microbiology and Molecular Genetics and Anatomy and Neurobiology, University of California, Irvine, CA 92697

[#] These authors contributed equally to this work.

Abstract

SCN1A mutations are the main cause of the epilepsy disorders Dravet syndrome (DS) and genetic epilepsy with febrile seizures plus (GEFS+). Mutations that reduce the activity of the mouse *Scn8a* gene, in contrast, are found to confer seizure resistance and extend the lifespan of mouse models of DS and GEFS+. To investigate the mechanism by which reduced *Scn8a* expression confers seizure resistance, we induced interictal-like burst discharges in hippocampal slices of heterozygous *Scn8a* null mice (*Scn8a*$^{med/+}$) with elevated extracellular potassium. *Scn8a*$^{med/+}$ mutants exhibited reduced epileptiform burst discharge activity after P20, indicating an age-dependent increased threshold for induction of epileptiform discharges. *Scn8a* deficiency also reduced the occurrence of burst discharges in a GEFS+ mouse model (*Scn1a*$^{R1648H/+}$). There was no detectable change in the expression levels of *Scn1a* ($Na_v1.1$) or *Scn2a* ($Na_v1.2$) in the hippocampus of adult *Scn8a*$^{med/+}$ mutants. To determine whether the increased seizure resistance associated with reduced *Scn8a* expression was due to alterations that occurred during development, we examined the effect of deleting *Scn8a* in adult mice. Global *Cre*-mediated deletion of a heterozygous floxed *Scn8a* allele in adult mice was found to increase thresholds to chemically and electrically induced seizures. Finally, knockdown of *Scn8a* gene expression in the adult hippocampus via lentiviral *Cre* injection resulted in a reduction in the number of EEG-confirmed seizures following the administration of picrotoxin. Our results identify the

[b]Correspondence to: Andrew Escayg; Department of Human Genetics, Emory University, Atlanta, GA 30322, USA; Tel.: 404-712-8328; Fax: 404-727-3949; aescayg@emory.edu, or Alan Goldin; Department of Microbiology and Molecular Genetics and Anatomy & Neurobiology; University of California, Irvine; Irvine, CA 92697-4025, USA; Tel.: 949-824-5334; Fax: 949-824-8504; agoldin@uci.edu..

Author contributions: C.D.M., B.S.T., A.E., and A.L.G. designed research; C.D.M., B.S.T., and T.L. conducted experiments; C.D.M., B.S.T., and T.L. analyzed data; C.D.M., B.S.T., A.E., and A.L.G. wrote the manuscript.

Author Declaration
The mouse model of GEFS+ described in this manuscript has been licensed to Allergan by Andrew Escayg. The terms of this arrangement have been reviewed and approved by Emory University in accordance with its conflict of interest policy. The remaining authors declare no competing financial interests.

hippocampus as an important structure in the mediation of *Scn8a*-dependent seizure protection and suggest that selective targeting of *Scn8a* activity might be efficacious in patients with epilepsy.

Introduction

Epilepsy is characterized by unprovoked, recurrent seizures that are manifestations of abnormal neuronal synchrony and excitability. Several genes that are known to cause monogenic forms of epilepsy encode neuronal ion channels, including voltage-gated sodium channels (VGSCs) (Noebels, 2003; Steinlein, 2004). VGSCs are important integrators of synaptic input and are responsible for the initiation and propagation of action potentials in neurons (Gong et al., 1999; Whitaker et al., 2001; Lorincz and Nusser, 2010). Three pore-forming VGSC α-subunit genes are primarily expressed in the adult mammalian central nervous system (CNS): *SCN1A*, *SCN2A*, and *SCN8A*, which encode the $Na_v1.1$, $Na_v1.2$, and $Na_v1.6$ channels, respectively. *SCN1A* has emerged as an important epilepsy gene and is responsible for a number of different epilepsy disorders, including the catastrophic, treatment-resistant childhood encephalopathy Dravet syndrome (DS) and genetic epilepsy with febrile seizures plus (GEFS+) (Escayg et al., 2000; Claes et al., 2001).

Approximately 30% of epileptic patients do not achieve adequate seizure control with currently available anti-epilepsy drugs (AEDs). Moreover, while new AEDs are generally better tolerated, the percentage of patients with treatment-resistant seizures has not changed significantly in the last 40 years, indicating a critical need to identify new treatment options for patients with refractory epilepsy. VGSCs are known targets for several AEDs; however, these drugs are not isoform specific and affect all VGSCs, likely contributing to unwanted side effects. Alternatively, selective targeting of a specific VGSC isoform, may provide improved seizure control with fewer unintended consequences.

We previously demonstrated that thresholds for flurothyl- and kainic acid-induced seizures are elevated in $Scn8a^{med/+}$ and $Scn8a^{medjo/+}$ mutant mice when compared to wild-type (WT) littermates (Martin et al., 2007). Furthermore, the seizure phenotypes of *Scn1a* mutant mice that model DS and GEFS+ were dramatically improved by the co-expression of an *Scn8a* mutation (Martin et al., 2007; Hawkins et al., 2011). In addition, *Scn8a*-deficient mice are resistant to amygdala kindling, while there is increased *Scn8a* expression in the CA3 region of the hippocampus of amygdala-kindled rats (Blumenfeld et al., 2009). Together, these studies raise the possibility that reduced hippocampal *Scn8a* expression may contribute to the seizure protection observed in $Scn8a^{med/+}$ mutants and that the selective targeting of *Scn8a* may be efficacious in some forms of epilepsy. However, a caveat of these earlier experiments is that the relationship between *Scn8a* and seizure resistance was based on the use of *Scn8a* mutant mice, in which the activity of *Scn8a* was reduced throughout brain development. Therefore, whether reduced *Scn8a* activity would confer seizure protection in the adult brain was unknown.

In this study, we examined the effect on seizure susceptibility of reducing *Scn8a* expression in adult mice. In addition to exploring the mechanism of seizure protection associated with altered *Scn8a* function, we used electrophysiological analysis to monitor developmental changes in hippocampal excitability in heterozygous $Scn8a^{med/+}$ mutants. Finally, using a

lentiviral-*Cre* strategy, we assessed the effect of reducing *Scn8a* expression in the adult hippocampus on seizures generated following the administration of picrotoxin.

Materials and Methods

Animals

C3HeB/FeJ-*Scn8a*^{med}/J mice (*Scn8a*$^{med/+}$, Jackson Laboratory, Bar Harbor, stock number 003798) were maintained on the C3HeB/FeJ background. The *med* mutation is the result of a spontaneous LINE element insertion in the second exon of the *Scn8a* gene leading to truncation and loss-of-function of the channel (Kohrman et al., 1996). *Scn8a*$^{med/+}$ male mice were crossed to C3HeB/FeJ females to generate *Scn8a*$^{med/+}$ and wild-type (WT) *Scn8a*$^{+/+}$ littermate controls. Mice expressing the UBC-Cre-ER^{T2} transgene (*ER-Cre*) were obtained from the Jackson Laboratory (stock number, 008085). *Scn8a*-floxed mice, in which exon 1 of the *Scn8a* gene is flanked by *loxP* sites (floxed allele), were a gift from Dr. Miriam Meisler at the University of Michigan, Ann Arbor (Levin and Meisler, 2004). The *ER-Cre* and *Scn8a*-floxed lines were maintained on the C57BL6/J background. Male *ER-Cre* mice were crossed to female *Scn8a*-floxed mice, producing progeny that express the floxed allele and the *ER-Cre* transgene (*flox/+*,*ER-Cre*). Controls consisted of offspring that express the floxed allele but lack the *ERCre* transgene (*flox/+*,no *Cre*), progeny that lack the floxed allele but carry the *Cre* transgene (*+/+*,*ER-Cre*), and progeny that lack the floxed allele and the *ER-Cre* transgene (*+/+*,no *Cre*). Vehicle-injected mice that carry both the floxed allele and the *ER-Cre* transgene were also used as controls (*flox/+*,*ER-Cre,* Veh.). Homozygous *Scn8a*-floxed mice that expressed the *ER-Cre* transgene *(flox/flox*,*ER-Cre*) were used to evaluate recombination efficiency. Homozygous floxed mice (*flox/flox*) were used for all experiments involving intrahippocampal viral *Cre* and *GFP* injections. *Scn1a*$^{R1648H/+}$ mice were generated as previously described (Martin et al., 2010). Double heterozygous mutants (*Scn1a*$^{R1648H/+}$,*Scn8a*$^{med/+}$) were generated by crossing *Scn1a*$^{R1648H/+}$ with *Scn8a*$^{med/+}$ mutant mice. All crosses yielded genotypes in expected Mendelian ratios. Littermates were used for all experiments to minimize confounds associated with differences in rearing conditions and genetic background. Experimenters were blinded to subject groups during data collection and analysis. Mice were maintained on a 12 h light/dark cycle. Food and water were available *ad libitum*. All experimental procedures were performed in accordance with the guidelines of Emory University and the University of California, Irvine Institutional Animal Care and Use Committees.

Genotyping

The presence of the *Cre* transgene and the *Scn8a* floxed allele was determined by PCR analysis using the primer pairs CreF/CreR (TGA CCC GGC AAA ACA GGT AGT TA / TTC CCG CAG AAC CTG AAG ATG TT) and FloxF/FloxR (GTG TGT GAT TCT CAA CAG TGG GTT / GTC TGT AAG AAG GCC TGA AAG TGA), respectively (Levin and Meisler, 2004). The *Scn8a*med mutation was identified as previously described (Martin et al., 2007) using the primer pair medF/medR (TCC AAT GCT TAT ACC AAA AGT CCC / GGA CGT GCA CAC TCA TTC CC). *Scn1a*$^{R1648H/+}$ mice were genotyped as previously described (Martin et al., 2010).

Tamoxifen-induced inactivation of Scn8a

Individually housed 2-month-old mice were intraperitoneally (i.p.) administered tamoxifen (TAM, 100 mg/kg, Sigma-Aldrich) or vehicle (corn oil, Sigma-Aldrich) for 5 consecutive days. TAM was prepared by dissolving in 100% ethanol and then mixing with 300 μl of corn oil. Excess ethanol was evaporated by vacuum centrifugation. Mice were left undisturbed for 15 days after the last injection.

Preparation and incubation of slices

Mice were anesthetized with halothane, decapitated, and their brains were placed in ice-cold sucrose artificial cerebrospinal fluid (ACSF) containing (in mM): 85 NaCl, 65 sucrose, 2.5 KCl, 25 glucose, 1.25 NaH_2PO_4, 4 $MgSO_4$, 0.5 $CaCl_2$, and 24 $NaHCO_3$. Transverse hippocampal slices (350 μm) were cut using a Leica VT1000S vibrating blade microtome (Leica, Germany). Slices were incubated at 33°C for at least 1 h before electrophysiological recordings in oxygenated (95% O_2, 5% CO_2) standard ACSF containing (in mM): 126 NaCl, 2.5 KCl, 1.25 $NaHPO_4$, 1.2 $MgSO_4$, 10 glucose, 1.2 $CaCl_2$, and 24 $NaHCO_3$.

Electrophysiological recordings

Slices were submerged in a recording chamber and continuously perfused at 2 mL/min with oxygenated ACSF at 33°C during electrophysiological experiments. Cells were visualized with an upright microscope (Zeiss Axioskop Plus) equipped with infrared differential interference contrast optics. Recording pipettes (2-5 MΩ) were pulled from borosilicate glass (Sutter Instruments, Novato, CA) with a P-87 Flaming-Brown puller (Sutter Instruments). Electrophysiological recordings were obtained in current clamp mode using MultiClamp 700B amplifier at 100X AC (Molecular Devices, Union City, CA) and digitized with a Digidata 1322A digitizer (Molecular Devices). Continuous extracellular recordings were acquired at 10 kHz and population spikes were recorded at 50 kHz. All recordings were low-pass filtered at 1 kHz for offline analysis with pClamp 10.2 software (Molecular Devices).

For extracellular recordings, pipettes were filled with 150 mM NaCl and positioned in the CA3 stratum pyramidal layer. ACSF with elevated potassium was prepared by supplementing standard ACSF with 3 M KCl to raise the potassium concentration to 8.5 mM $[K^+]_O$. The experimental paradigm consisted of a control recording for 2-5 min in standard ACSF, followed by 20-25 min with 8.5 mM $[K^+]_O$, in which burst activity was recorded. To evoke population spikes, constant-current stimuli (100 μsec) were applied via stimulus isolator (A365D; WPI, Sarasota, FL) using a bipolar tungsten electrode (50μm in diameter; A-M Systems, Carlsborg, WA) positioned in the mossy fiber tract. Population spikes were evoked in physiological 2.5 mM $[K^+]_O$ before and after exposing the slice to 8.5 mM $[K^+]_O$. Slices in which population spike amplitudes did not change more than 20% after exposing the slice to 8.5 mM $[K^+]_O$ were used for analysis.

Protein extraction

Hippocampi were dissected and frozen at −80°C. To determine developmental changes in *Scn8a* expression, individual hippocampi were pooled from 10-15 mice at each age.

Hippocampi from adult, 2-3-month-old, mice were not pooled. Hippocampi were homogenized on ice using a Dounce homogenizer in homogenization buffer (320 mM sucrose, 5 mM Na phosphate, pH 7.4, 100 mM Na fluoride and protease inhibitor (Pierce, Rockford, IL) or 50 mM Tris, pH = 7.5; 10 mM EGTA, and one complete EDTA-free protein inhibitor tablet (Roche, Germany) per 50 mL solution. Homogenates were centrifuged at 750 × g for 10 min at 4°C, and the supernatant was centrifuged at 39,000 × g for 30 or 60 min at 4°C. The pellet was suspended in protease inhibitor buffer and stored at −80°C. BCA (Thermo Fisher Scientific, Waltham, MA) or Bradford (Bio-Rad, Hercules, CA) protein assays were used to normalize protein concentrations across samples.

Western blot analysis

Membrane-enriched whole-brain or hippocampal tissue homogenates (15-30 ug) were subjected to SDS-PAGE electrophoresis. After blocking in 5% milk, blots were incubated overnight at 4°C in either polyclonal rabbit anti-$Na_v1.6$ primary antibody (1:200, Millipore, Billerica, MA), polyclonal rabbit anti-$Na_v1.6$ (1:225, Alomone, Israel), polyclonal rabbit anti-$Na_v1.1$ (1:200, Millipore), or monoclonal mouse anti-$Na_v1.2$ (1:1000, Neuromab, Davis, CA). Blots were then incubated in either HRP-conjugated donkey anti-rabbit secondary (1:10,000, GE Healthcare, United Kingdom), HRP-conjugated goat anti-mouse secondary (1:10,000, Jackson ImmunoResearch, West Grove, PA), or HRP-conjugated goat anti-rabbit secondary (Sigma, St. Louis, MO, 1:16,000) for 1 h followed by washing in SuperSignal West Pico Chemiluminescent substrate (Pierce) and imaging. Blots were also probed using a monoclonal mouse anti-α-tubulin (1:10,000, Millipore) or monoclonal mouse anti-pan-cadherin (1:100,000, Sigma) antibody followed by HRP-conjugated goat anti-mouse secondary (1:10,000, Jackson ImmunoResearch) or HRP-conjugated goat anti-mouse secondary (Pierce, 1:26,000) for normalization of sample loading. Image quantification was performed using ImageJ software (NIH).

Quantitative real-time PCR

Total RNA was extracted from the hippocampus of WT and *Scn8a*$^{med/+}$ adult mice using the RNeasy Lipid Tissue Mini Kit (Qiagen, Germany). All RNA samples were quantified using a NanoDrop 1000 Spectrophotometer (Thermo Fisher Scientific), and RNA quality was determined by agarose gel electrophoresis. RNA was reverse-transcribed into cDNA using random hexamer primers and SuperScript III reverse transcriptase (Invitrogen, Carlsbad, CA). *Scn1a* (F: TCAGGAGGAAGGGGTTTCGCTTC, R: CCCCACATCCTTGGCTCGCCCTC) and *Scn2a* (F: CTGCAACGGTGTGGTCTCCCTAG, R: ATGTAGGGTCTTCCAACAAGTCC) primers were designed to span introns to avoid amplification of genomic DNA. Each primer pair generated standard curves with efficiencies of 90-100%. Real-time PCR (qPCR) data were generated from cDNA samples in technical triplicate using the BioRad CFX96 Real-Time PCR Detection System and SYBR Green fluorescent dye (BioRad). Expression levels were normalized to beta-actin (F: CAGCTTCTTTGCAGCTCCTT, R: ACGATGGAGGGGAATACAGC). Expression analysis and statistics were performed using the GenEx 5 software (MultiD).

Lentiviral constructs and virus

Previously described viral vectors expressing green fluorescent protein (LV-*GFP*) or *Cre*recombinase (LV-*Cre*) were obtained from the Emory University Viral Core (Heldt et al., 2007). Briefly, LV-*GFP* viral vectors were derived from the pLV-CMV-GFP-U3Nhe backbone. LV-*Cre* viral vectors were created by replacing the *GFP* coding sequence with *Cre*-recombinase coding sequence using the BamH1/Sal1 restriction sites in the pLV-CMV-GFP-U3he backbone. Viral production procedures have been described previously (Miyoshi et al., 1998; Pfeifer et al., 2001). Viral titer of the LV-*GFP* and LV-*Cre* was assessed in HEK-293T cells and ranged from 1×10^8 to 1×10^9 infectious particles per ml.

Surgical procedures

Surgical implantation of EEG electrodes was performed as previously described (Martin et al., 2007; Dutton et al., 2012; Papale et al., 2013). Mice were anesthetized by isoflurane inhalation, and then fixed in a stereotaxic apparatus (Kopf, Tujunga, CA). Four holes were drilled in the skull above each injection site. Injections were performed using a Hamilton 0.5-μl microsyringe (model #75) and 30-gauge needle. Four injection sites were chosen to target the hippocampus at the following coordinates, from bregma: anteroposterior (AP), -1.9 mm; mediolateral (ML), ±1.1 mm, ±2.1 mm; dorsoventral (DV), -1.9 mm. The syringe was lowered to -2.0 mm, and then retracted to -1.9 mm and left in place for 4 min. Virus solution (1.0 μl) was injected into each site at a rate of 0.12 μl/min. After each injection, the syringe was left in place for 4 minutes before being retracted. Following viral injections, 4 sterile cortical screw electrodes (Vintage Machine Supplies, OH) were implanted subdurally in the skull for EEG recordings at the following coordinates, from bregma: 1.5 mm (AP) and +2.1 mm ML; -1.9 mm AP and ±2.1 mm ML; 0.5 mm AP and -2.1 mm ML. Fine-wire electrodes were implanted into the neck muscle for EMG acquisition. Incisions were closed with tissue adhesive (Vetbond, 3M; St. Paul, NM), and the animal was allowed to recover on a heating pad. Postoperative analgesic (ibuprofen, 0.1 mg/kg) was provided for 3 days in the drinking water.

Histological procedures

Mice were anesthetized using isoflurane and transcardially perfused with 4% paraformaldehyde (PFA) 15-20 d following LV-*GFP* injection. Brains were post-fixed for 2 h in ice-cold 4% PFA, and then transferred to 30% sucrose for 3 d at 4°C. Coronal sections (45 μm) were sliced using a cryostat (Leica) between bregma -1.0 mm and -4.0 mm. Sections were washed in TBS/Triton-X and mounted. Images were collected using a Leica DM6000 B upright fluorescence microscope and Simple PCI software.

Seizure induction paradigms

Flurothyl seizure induction—Flurothyl seizure induction was performed as previously described (Martin et al., 2007; Martin et al., 2010). Briefly, 3-month-old mice were placed in a clear Plexiglas chamber. Flurothyl (2,2,2-trifluroethyl ether, Sigma-Aldrich) was introduced at a rate of 20 μl/min. The latencies to the first myoclonic jerk (MJ) and generalized tonic-clonic seizure (GTCS) were recorded. The MJ was defined as a jerking movement of the neck and shoulders sometimes associated with tail clonus. The GTCS was

defined as complete loss of postural control associated with forelimb and hindlimb tonic-clonic movement lasting longer than 3 s.

Kainic acid (KA) seizure induction—Three-month-old mice were administered KA (i.p., 25 mg/kg, Sigma-Aldrich) and observed for 2 h. The latency to the first occurrence of each event on a modified Racine scale was recorded: 1 = freezing, 2 = head nodding, 3 = tail clonus, 4 = forelimb clonus, 5 = rearing and falling, 6 = GTCS. The GTCS was defined as complete loss of postural control associated with forelimb and hindlimb tonic-clonic movement lasting longer than 3 s.

6-Hz psychomotor seizure induction—A brief electric current (6-Hz, 26 mA, 3-ms pulse width, 3-s duration) was applied to the cornea of 3-month-old mice (Ugo Basile S.R.L, Germany). Seizure severity was recorded using the following modified Racine scale: 1 = staring, 2 = forelimb clonus, 3 = rearing and falling. Mice that did not exhibit seizure activity in response to the first exposure were excluded from the study and did not proceed to receive TAM or vehicle. Those mice that exhibited seizure activity were placed into two groups for TAM or vehicle administration. These groups were balanced based on seizure severity to ensure that seizure susceptibility was comparable between groups before administration of TAM or vehicle. TAM or vehicle injections were initiated one day after the first current exposure. Two weeks after the last TAM injection, the mice underwent 6-Hz seizure induction a second time.

Picrotoxin (PT) seizure induction—. Fifteen days following either LV-*Cre* or LV-*GFP* hippocampal injection and surgical EEG implantation, PT seizure induction was performed as previously described (Distler et al., 2013). Video/EEG recordings were collected and amplified using the Stellate Harmony System and software (Natus Medical, Inc., San Carlos, CA). Signals were filtered (EEG 0.3-35 Hz bandpass, EMG 10-70 Hz bandpass) and digitized at a sampling rate of 200 Hz. Twenty min of baseline video/EEG recording was collected before administering PT. Following PT administration (i.p., 10 mg/kg, Sigma-Aldrich), the latency to the first seizure, duration of each seizure, and number of seizures were recorded. Seizures were defined behaviorally by the presence of generalized convulsions and confirmed by the presence of highly synchronous EEG activity that reached at least twice the baseline amplitude in all cortical EEG channels and persisted for at least 3 s. Video/EEG monitoring was performed for at least 2 h following PT administration.

Statistics

All bar graphs indicate the mean and all error bars represent ± standard error of the mean (SEM). Statistical analyses were performed using SigmaPlot 11.0 software (Systat Software Inc., Chicago, IL), Prism 6 (GraphPad Software Inc, La Jolla, CA), and GenEx 5 software (Multi D). The Levene's test was used to assess for differences in the variance between groups, and the Shapiro-Wilk test was used to determine normality of continuous data sets. One-way analysis of variance (ANOVA) was used to evaluate seizure thresholds between ER-*Cre* groups treated with flurothyl. Two-way analysis of variance (ANOVA) was used to evaluate KA seizure thresholds. *Post-hoc* comparisons were performed using either the Dunnett's or Bonferroni test. The Student's two-tailed t test was used to analyze the

percentage knockdown of *Scn8a* protein levels by the ER-*Cre* transgene and by LV-*Cre* injection, as well as to compare qPCR results between genotypes for each sodium channel. qPCR expression analysis and statistics were performed using the GenEx 5 software. Student's two-tailed t test was also used to determine the significance of burst discharge latency, duration, and frequency, and Fisher's exact test with Bonferroni correction was used to compare the occurrence of burst discharges. Fisher's exact test was used to assess categorical seizure outcomes following 6-Hz seizure induction. The Mann-Whitney-U test was used to assess PT seizure outcomes.

Results

Epileptiform burst discharge activity is reduced in *Scn8a*$^{med/+}$ mutant mice

Since the hippocampus is known to play an important role in seizure generation, we examined temporal changes in the excitability of hippocampal slices from heterozygous *Scn8a* null mutant mice (*Scn8a*$^{med/+}$). Epileptiform burst discharges were induced in the CA3 pyramidal cell layer of the hippocampus by elevating the extracellular potassium concentration (Fig. 1*Aa-c*). Burst discharges were not observed during the initial 5 minutes at physiological potassium concentration (2.5 mM $[K^+]_o$) in hippocampal slices from either WT (Fig. 1*Aa*) or *Scn8a*$^{med/+}$ mutant mice (Fig. 1*B*). However, elevating the extracellular K^+ concentration to 8.5 mM induced synchronous burst discharge activity in hippocampal slices from most WT mice at all ages (P13-P84) (Fig. 1*A,D*). Individual burst discharges were composed of a positive extracellular potential with multiple population spikes (Fig. 1*Ac*). Burst activity continued until the extracellular K^+ was returned to physiological concentration (2.5 mM). Similarly, hippocampal slices from young P13-P20 *Scn8a*$^{med/+}$ mutant mice displayed burst discharges when exposed to elevated potassium (Fig. 1*D*). In contrast, burst discharges were not observed in the majority of slices from *Scn8a*$^{med/+}$ mutant mice older than P20 (Fig. 1*B,D*). The lack of activity was not due to poor health of the cells because synaptic connections and neuronal firing remained intact, as determined by stable population spike amplitudes in the CA3 pyramidal layer before and after exposure to elevated potassium (Fig. 1*C*). The frequency of observed epileptiform burst discharges was lower in more mature WT mice (P26 and P70-84), but was still comparably much higher than that observed in slices from *Scn8a*$^{med/+}$ mutant mice (Fig. 1*D*). For example, burst discharges were observed in 86% of slices from adult WT mice, but in only 12% of slices from adult *Scn8a*$^{med/+}$ mice (P70-84).

Latency to burst discharges is increased in *Scn8a*$^{med/+}$ mutant mice

Because $Na_v1.6$ channels are well suited for repetitive firing of action potentials and hence hyperactivity of the neuronal network, we compared the latency to the initiation of burst discharges in slices from *Scn8a*$^{med/+}$ mutants and WT littermates. Latency to the initial burst discharge was measured from the time that elevated potassium ACSF entered the recording chamber. *Scn8a*$^{med/+}$ mutant mice in all 3 age groups tested displayed a significant increase in the latency to the initiation of epileptiform burst activity (Fig. 2*A*). However, once burst discharge activity was induced, there were no qualitative differences in the pattern of synchronous activity. To determine whether there were any quantitative differences in burst activity, we analyzed the inter-burst frequency and single burst duration. Because the

majority of hippocampal recordings from *Scn8a*$^{med/+}$ mutant mice did not exhibit burst activity (Fig. 1*D*), only hippocampal slices from the few *Scn8a*$^{med/+}$ mutant mice that produced burst discharges were used for this analysis. Inter-burst frequency was measured as the number of burst discharges during a 4-min period, and burst duration was determined from an average of 50 individual bursts (Fig. 1*Ac*). There were no significant differences in either the inter-burst frequency or single burst duration between *Scn8a*$^{med/+}$ mutant and WT mice in all 3 age groups examined (Fig. 2*B-C*).

Reduced *Scn8a* expression decreases the occurrence of burst discharges in *Scn1a*$^{R1648H/+}$ mice

To investigate whether reduced *Scn8a* expression could alter the occurrence of epileptiform burst discharges in a mouse model of GEFS+ (*Scn1a*$^{R1648H/+}$ mice), we generated double heterozygous mutants (*Scn1a*$^{R1648H/+}$/*Scn8a*$^{med/+}$) and quantitatively examined burst activity in hippocampal slices exposed to elevated potassium. Burst occurrence, defined as the number of slices that exhibited bursting, was significantly lower in slices from *Scn8a*$^{med/+}$ and double heterozygous mice compared to WT (Table 1). Burst occurrence was also significantly reduced in double heterozygous mice compared to *Scn1a*$^{R1648H/+}$ mice (Table 1). While burst occurrence was comparable in slices from *Scn1a*$^{R1648H/+}$ mutants and WT littermates, burst latency was significantly shorter in *Scn1a*$^{R1648H/+}$ mice. An increase in inter-burst frequency was also observed in slices from *Scn1a*$^{R1648H/+}$ mutants compared to WT; however, this difference was not statistically significant. It was not possible to statistically evaluate burst latency or frequency in slices from *Scn8a*$^{med/+}$ mice (with or without the *Scn1a*$^{R1648H/+}$ mutation) because of the low percentage of hippocampal slices that demonstrated burst activity. However, increased latencies to bursting and decreased inter-burst frequencies were observed in *Scn8a*$^{med/+}$ slices (with or without the *Scn1a*$^{R1648H/+}$ mutation) compared to *Scn1a*$^{R1648H/+}$ slices in the few instances in which bursting occurred.

Developmental expression profile of Na_v 1.6 channels in the hippocampus

Because decreased burst activity was seen only in slices from *Scn8a*$^{med/+}$ mutant mice older than P20, we investigated whether this decrease was correlated with changes in developmental expression of $Na_v1.6$ channels by performing Western blot analysis. $Na_v1.6$ was detectable in the hippocampus as early as P10 and progressively increased until adult levels were reached between 3-4 weeks after birth (Fig. 3A). A high level of $Na_v1.6$ expression is observed at P18 prior to the time-point (P21) at which decreased burst activity is observed. To determine whether reduced *Scn8a* expression in *med* mutants is associated with altered levels of other VGSC alpha subunits, we compared *Scn1a* and *Scn2a* mRNA and protein levels from hippocampi of 3-month-old *Scn8a*$^{med/+}$ and WT littermates. Consistent with previous observations (Kearney et al., 2002), we found no significant differences in expression levels (Fig. 3 *B-C*).

Cre recombinase induction leads to deletion of the floxed allele and reduced Na_v 1.6 levels

To examine the effect of reducing *Scn8a* expression on seizure thresholds in adult mice, we crossed a tamoxifen (TAM)-inducible *Cre* line (*ER-Cre)* with *Scn8a* floxed mice to generate

progeny in which inactivation of the *Scn8a* gene could be achieved by TAM injection. PCR analysis performed on hippocampal tissue from *flox/+,ER-Cre* mice 15 d after the last TAM injection detected a 300-bp PCR band, indicating deletion of exon 1 of the *Scn8a* gene (Fig. 4*A*). This PCR product was not observed in mice that were not administered TAM, or in mice that either lacked the floxed *Scn8a* allele or the *Cre* transgene (Fig. 4*A*). Reduced optical density (78% reduction) of the *Scn8a* band by Western blot analysis demonstrated reduced expression of the $Na_v1.6$ protein in *flox/flox,ER-Cre* mice that were administered TAM compared to *flox/flox,ER-Cre* mice that were administered vehicle (Fig. 4*B-C*).

Inactivation of *Scn8a* leads to increased resistance to chemically and electrically induced seizures

Latencies to flurothyl-induced seizures following TAM-induced inactivation of the *Scn8a* allele were compared between *Scn8a*-deficiant animals (*flox/+,ER-Cre*,TAM) (white bar, Fig. 5*A*) and control littermates with normal levels of *Scn8a* (+/+,no *Cre*,TAM; +/+,ER-*Cre*,TAM; *flox/+*,no *Cre*,TAM; and *flox/+,ER-Cre*,Veh) (black bars, Fig. 5*A*). Myoclonic jerk latency was reduced in +/+,ER-*Cre*,TAM; *flox/+*,no *Cre*,TAM; and *flox/+,ER-Cre*,Veh animals but not +/+,no Cre,TAM mice compared to *flox/+,ER-Cre*,TAM animals. Significantly increased latencies to the GTCS were observed between *Scn8a*-deficient mice when compared to all control groups (Fig. 5*A*).

Latencies to KA-induced seizures were also compared between *Scn8a*-deficient (*flox/+,ERCre*,TAM) mice and control (*flox/+,ER-Cre*,Veh) mice. Latency to the first occurrence of each seizure stage on a modified Racine scale was recorded. Significantly increased latencies to stage 5 and stage 6 were observed in the *flox/+,ER-Cre*,TAM mice when compared to control littermates (Fig. 5*B*).

The 6-Hz model of psychomotor seizures was used to determine the effect of reducing *Scn8a* expression on electrically induced seizures. The severity of evoked seizures in $Scn8a^{flox/+}$,*ER-Cre* mice before and after TAM or vehicle administration was recorded using a modified Racine scale. A significant reduction in seizure severity was observed after TAM injection but not after vehicle injection (Fig. 5*C*). A trend toward a reduction in the percentage of mice exhibiting seizure activity was also observed following TAM administration, with 43% (3/7) of mice exhibiting seizures after TAM administration, compared to 89% (8/9) of mice exhibiting seizures after vehicle administration (Fig. 5*D*).

Lentiviral *Cre*-induced inactivation of the *Scn8a* gene in the hippocampus reduces seizure generation *in vivo*

To determine whether restricting *Scn8a* inactivation to the hippocampus would be sufficient to increase seizure resistance *in vivo*, LV-*Cre* or LV-*GFP* were injected into the hippocampus of *flox/flox* mice. *GFP*-positive cells were observed in the CA1, CA3, and DG layers of the hippocampus with highest expression in the DG and CA3 (Fig. 6*A*). Responses to picrotoxin (PT) were measured 15 days after injection of the lentiviral constructs. We observed a statistically significant reduction in the number of seizures in LV-*Cre*-injected mice compared to LV-*GFP*-injected controls (Fig. 6*B*); however, the average latency to the first seizure and the average seizure length were not significantly altered (Fig. 6*C-D*).

Representative EEG recordings of baseline and seizure activity are shown for LV-*GFP*-injected controls and LV-*Cre*-injected mice (Fig. 6*E*).

Discussion

Previous studies examining the relationship between *Scn8a* and seizure resistance relied on the use of mice that expressed *Scn8a* mutations throughout development. To determine whether seizure protection would also be observed if *Scn8a* expression was reduced only in the adult brain, we used a TAM-inducible *Cre* transgenic line to initiate the inactivation of a floxed *Scn8a* allele in adult mice. We found that global reduction of *Scn8a* expression in the adult brain was capable of raising latencies to flurothyl- and KA-induced seizures. In addition, we found that reduced *Scn8a* expression in adult mice increased resistance to 6-Hz psychomotor seizures, a paradigm used to screen for novel anti-epileptic drugs (Brown, 1953; Barton et al., 2001). These results show that seizure protection can be achieved by reducing *Scn8a* expression in the adult brain, which is a critical requirement for an anticonvulsant therapy. This finding and the other main results of this study are summarized in Table 2.

To test the hypothesis that reduced *Scn8a* expression leads to reduced hippocampal excitability and seizure suppression, we studied hippocampal slices from *Scn8a*$^{med/+}$ and WT littermates in a high-potassium model of epileptiform activity throughout postnatal development. We found that *Scn8a*$^{med/+}$ hippocampal slices were resistant to interictal-like burst discharges beginning at P20. There was an increase in the latency to epileptiform burst discharges in *Scn8a*$^{med/+}$ slices, suggesting that reduced *Scn8a* expression inhibits the initiation of bursting activity; however, there were no changes in inter-burst frequency or single burst duration relative to slices from WT mice. Our data indicate that there is a deficiency in epileptiform burst discharge initiation but not burst discharge propagation since epileptiform activity progresses comparably between WT and *Scn8a*-deficient slices following initiation. Additionally, the abrupt reduction in burst percentage in *Scn8a*-deficient slices at P21 is remarkable and cannot fully be explained by developmental changes in *Scn8a* expression which occurs over the course of several weeks. P21 in the mouse corresponds to a developmental stage at which neuronal excitability is likely to be influenced by a number of processes. For example, $Na_v1.6$ replaces $Na_v1.2$ during this time period and myelination is at a maximum at postnatal day 20 (Norton and Poduslo, 1973). We speculate that the effect of these changes on neuronal excitability in combination with reduced *Scn8a* activity likely contributes to the abrupt reduction in neuronal excitability in *Scn8a*-deficient animals.

$Na_v1.6$ channels have characteristic biophysical properties, including persistent current, resurgent current, and resistance to inactivation, which makes this isoform well suited for the sustained high-frequency firing that occurs at the axon initial segment and nodes of Ranvier, but may also allow this channel to facilitate the propagation of high-frequency ictal activity (Raman et al., 1997; Zhou and Goldin, 2004). Despite these unique characteristics, *Scn8a*$^{med/+}$ mutant mice showed no significant changes in inter-burst frequency or single burst duration. It is possible that there are changes in action potential firing that we could not detect because they are below the sensitivity of our assay; or, it may be that the decreased

seizure activity is a property of the overall network and therefore does not reflect simple changes in bursting in any one region. Prior studies have shown that mice with altered *Scn8a* expression have reduced persistent current and depolarized action potential spike thresholds in hippocampal pyramidal neurons that may impede the firing of repetitive action potentials (Royeck et al., 2008; Blumenfeld et al., 2009). These biophysical changes are consistent with the longer latency to the initial burst discharge and higher seizure threshold in *Scn8a*$^{med/+}$ mutants. These results suggest that reduced *Scn8a* expression leads to reduced hippocampal network excitability and consequently reduced susceptibility to epileptiform activity. We also demonstrated that reduced *Scn8a* expression suppresses the occurrence of burst discharges in the hippocampus of *Scn1a*$^{R1648H/+}$ mice thereby providing a mechanistic basis for our previous observations of ameliorated seizure phenotypes in *Scn1a* mutant mice that co-express *Scn8a* mutations (Martin et al., 2007; Hawkins et al., 2011).

Parallel to our measurement of hippocampal bursting activity throughout early postnatal development, we also examined developmental changes in the expression levels of $Na_v1.6$ in the hippocampus. Consistent with previous observations, Western blot analysis revealed that $Na_v1.6$ is detectable by P10 and reaches adult levels by the third postnatal week (Plummer et al., 1997; Liao et al., 2010). Also, consistent with previous reports (Kohrman et al., 1996; Vega et al., 2008), we observed reduced *Scn8a* expression in *Scn8a*$^{med/+}$ mutants compared to WT littermates (data not shown). The emergence of reduced epileptiform burst discharges in *Scn8a*$^{med/+}$ mice coincided with the beginning of the developmental period in which *Scn8a* is highly expressed, and therefore likely to significantly influence neuronal excitability. This suggests that the reduced epileptiform bursting in *Scn8a*$^{med/+}$ mice is, in part, a consequence of lower *Scn8a* expression levels during this period. The expression levels of *Scn1a* ($Na_v1.1$) and *Scn2a* ($Na_v1.2$) were unaltered in the hippocampi of adult *Scn8a*$^{med/+}$ mutants, which is consistent with previously reported observations on *Scn8a*$^{medJ/medJ}$ mice which have a 90% reduction in $Na_v1.6$ expression (Kearney et al., 2002).

Previous studies examining *Scn8a*-mediated seizure resistance raised the possibility of a self-reinforcing relationship between *Scn8a* expression and neuronal activity in which increases in neuronal activity lead to increased *Scn8a* expression, which in turn further increases neuronal excitability in the CA3 region of the hippocampus and contributes to epilepsy (Blumenfeld et al., 2009). Genetically reducing *Scn8a* expression might block this positive feedback cycle. An additional possibility is that *Scn8a* localization at the proximal axon initial segment of hippocampal dentate gyrus neurons places these channels in a prime location to regulate the low-pass filtering capability of these neurons, which is thought to help protect the hippocampus from seizure activity (Hsu, 2007; Kress et al., 2010). Furthermore, dentate gyrus neurons express comparatively lower levels of *Scn8a* when compared to CA3 (Kress et al., 2010), perhaps making their intrinsic excitability more sensitive to changes in *Scn8a* expression. These results, together with our findings, indicate that the hippocampus is a key region for *Scn8a*-mediated seizure resistance.

To directly test the hypothesis that targeting *Scn8a* in the hippocampus is sufficient to increase seizure resistance, we performed lentiviral-*Cre* and *GFP* injections into the hippocampus of conditional *Scn8a* mice (*flox/flox*) and measured response to PT

administration. This approach resulted in an overall 14% reduction in $Na_v1.6$ levels in the hippocampus (data not shown). GFP positive cells were detected in the CA3, dentate gyrus and dentate hilus regions of the hippocampus while few targeted cells in CA1 were identified. Hippocampal knockdown of *Scn8a* led to a significant reduction in the number of electrographic seizures resulting from PT administration. However, the latency to the first electrographic seizure and the average duration of all seizure events were comparable between LV-*GFP* and LV-*Cre* groups. This finding indicates that the hippocampus is an important regulator of *Scn8a*-dependent CNS excitability and supports the possibility that targeting of *Scn8a* may provide an efficacious treatment for some forms of epilepsy. Furthermore, we speculate that reduction of *Scn8a* expression in the CA3 and DG hippocampal regions is primarily responsible for the observed seizure protection as reducing sodium channel expression in inhibitory neurons of the dentate hilus is not likely to lead to seizure protection.

Although heterozygous *Scn8a* null mice (*Scn8a*$^{med/+}$) are visibly normal, they exhibit anxiety-like behavior and have spike-wave discharges that are characteristic of absence seizures (Burgess et al., 1995; McKinney et al., 2008; Papale et al., 2009). In one human family, *SCN8A* haploinsufficiency was associated with cognitive deficits (Trudeau et al., 2006). Additional studies will therefore be required to evaluate the effects on behavior and cognition of targeting *Scn8a* in epileptic animals. It is possible that normalizing the excitability of an epileptic region by targeting *Scn8a* will not result in the behavioral deficits that may occur when *Scn8a* is reduced in an otherwise normal animal. In addition, restricted targeting of *Scn8a* may reduce the likelihood of unwanted consequences. In support of this hypothesis, mice with hippocampal knockdown of *Scn8a* displayed normal visible behavior and no absence seizures during video/EEG recordings.

The *SCN8A* mutation N1786D was recently identified in a patient with severe epilepsy, cognitive deficits, and sudden unexpected death in epilepsy (SUDEP) (Veeramah et al., 2012). In addition, loss of the RNA-binding protein Celf4 has been shown to lead to an increase in *Scn8a* expression and to spontaneous seizure generation in mice (Sun et al., 2013). These findings seem to contradict observed improvements in seizure protection in *Scn8a* mutant mice. However, the available mouse models of *Scn8a* dysfunction have reduced sodium currents, whereas the N1786D is a gain-of-function mutation with increased persistent current (Veeramah et al., 2012), and Celf4 deficiency is believed to result in increased $Na_v1.6$ expression at the axon initial segment and increased persistent current (Sun et al., 2013). Thus, reduced $Na_v1.6$ currents likely lead to reduced neuronal excitability and seizure protection, whereas alterations that increase $Na_v1.6$ currents, in particular those that increase persistent current, lead to greater neuronal excitability and seizure susceptibility.

Conclusions

We have determined that hippocampal $Na_v1.6$ is an important regulator of neuronal excitability and seizure susceptibility. These results raise the possibility that targeting *Scn8a*, either genetically or with $Na_v1.6$ specific compounds, may be an efficacious treatment strategy for some forms of epilepsy.

Acknowledgments

Research in this publication was supported by the National Institute of Neurological Disorders and Stroke (NINDS) of the National Institutes of Health (NIH) under award numbers R01NS072221 (A.E.), R01NS048336 (A.L.G.), R01NS065187 (A.E. and A.L.G.), and F31NS074717 (C.D.M). The content is solely the responsibility of the authors and does not necessarily represent the official views of the NIH. We would like to thank the Emory University Viral Core for assistance with reagents and Dr. Miriam Meisler for providing the *Scn8a* floxed line. We would also like to thank Karoni Dutt and Eric Velazquez for helpful discussions during the course of this work and Cheryl Strauss for editorial assistance.

Reference List

Barton ME, Klein BD, Wolf HH, White HS. Pharmacological characterization of the 6 Hz psychomotor seizure model of partial epilepsy. Epilepsy research. 2001; 47:217–227. [PubMed: 11738929]

Blumenfeld H, Lampert A, Klein JP, Mission J, Chen MC, Rivera M, Dib-Hajj S, Brennan AR, Hains BC, Waxman SG. Role of hippocampal sodium channel Nav1.6 in kindling epileptogenesis. Epilepsia. 2009; 50:44–55. [PubMed: 18637833]

Brown CW. Properties and Alterations of Electrically-Induced Seizures in Mice. Epilepsia. 1953; C2:127–138.

Burgess DL, Kohrman DC, Galt J, Plummer NW, Jones JM, Spear B, Meisler MH. Mutation of a new sodium channel gene, Scn8a, in the mouse mutant 'motor endplate disease'. Nat Genet. 1995; 10:461–465. [PubMed: 7670495]

Claes L, Del-Favero J, Ceulemans B, Lagae L, Van Broeckhoven C, De Jonghe P. De novo mutations in the sodium-channel gene SCN1A cause severe myoclonic epilepsy of infancy. American journal of human genetics. 2001; 68:1327–1332. [PubMed: 11359211]

Distler MG, Gorfinkle N, Papale LA, Wuenschell GE, Termini J, Escayg A, Winawer MR, Palmer AA. Glyoxalase 1 and its substrate methylglyoxal are novel regulators of seizure susceptibility. Epilepsia. 2013; 54:649–657. [PubMed: 23409935]

Dutton SB, Makinson CD, Papale LA, Shankar A, Balakrishnan B, Nakazawa K, Escayg A. Preferential inactivation of Scn1a in parvalbumin interneurons increases seizure susceptibility. Neurobiol Dis. 2012; 49C:211–220. [PubMed: 22926190]

Escayg A, MacDonald BT, Meisler MH, Baulac S, Huberfeld G, An-Gourfinkel I, Brice A, LeGuern E, Moulard B, Chaigne D, Buresi C, Malafosse A. Mutations of SCN1A, encoding a neuronal sodium channel, in two families with GEFS+2. Nature genetics. 2000; 24:343–345. [PubMed: 10742094]

Gong B, Rhodes KJ, Bekele-Arcuri Z, Trimmer JS. Type I and type II Na(+) channel alpha-subunit polypeptides exhibit distinct spatial and temporal patterning, and association with auxiliary subunits in rat brain. The Journal of comparative neurology. 1999; 412:342–352. [PubMed: 10441760]

Hawkins NA, Martin MS, Frankel WN, Kearney JA, Escayg A. Neuronal voltage-gated ion channels are genetic modifiers of generalized epilepsy with febrile seizures plus. Neurobiol Dis. 2011; 41:655–660. [PubMed: 21156207]

Heldt SA, Stanek L, Chhatwal JP, Ressler KJ. Hippocampus-specific deletion of BDNF in adult mice impairs spatial memory and extinction of aversive memories. Mol Psychiatry. 2007; 12:656–670. [PubMed: 17264839]

Hsu D. The dentate gyrus as a filter or gate: a look back and a look ahead. Prog Brain Res. 2007; 163:601–613. [PubMed: 17765740]

Kearney JA, Buchner DA, De Haan G, Adamska M, Levin SI, Furay AR, Albin RL, Jones JM, Montal M, Stevens MJ, Sprunger LK, Meisler MH. Molecular and pathological effects of a modifier gene on deficiency of the sodium channel Scn8a (Na(v)1.6). Hum Mol Genet. 2002; 11:2765–2775. [PubMed: 12374766]

Kohrman DC, Harris JB, Meisler MH. Mutation detection in the med and medJ alleles of the sodium channel Scn8a. Unusual splicing due to a minor class ATAC intron. The Journal of biological chemistry. 1996; 271:17576–17581. [PubMed: 8663325]

Kress GJ, Dowling MJ, Eisenman LN, Mennerick S. Axonal sodium channel distribution shapes the depolarized action potential threshold of dentate granule neurons. Hippocampus. 2010; 20:558–571. [PubMed: 19603521]

Levin SI, Meisler MH. Floxed allele for conditional inactivation of the voltage-gated sodium channel Scn8a (NaV1.6). Genesis. 2004; 39:234–239. [PubMed: 15286995]

Liao Y, Deprez L, Maljevic S, Pitsch J, Claes L, Hristova D, Jordanova A, Ala-Mello S, Bellan-Koch A, Blazevic D, Schubert S, Thomas EA, Petrou S, Becker AJ, De Jonghe P, Lerche H. Molecular correlates of age-dependent seizures in an inherited neonatal-infantile epilepsy. Brain : a journal of neurology. 2010; 133:1403–1414. [PubMed: 20371507]

Lorincz A, Nusser Z. Molecular identity of dendritic voltage-gated sodium channels. Science. 2010; 328:906–909. [PubMed: 20466935]

Martin MS, Tang B, Papale LA, Yu FH, Catterall WA, Escayg A. The voltage-gated sodium channel Scn8a is a genetic modifier of severe myoclonic epilepsy of infancy. Hum Mol Genet. 2007; 16:2892–2899. [PubMed: 17881658]

Martin MS, Dutt K, Papale LA, Dube CM, Dutton SB, de Haan G, Shankar A, Tufik S, Meisler MH, Baram TZ, Goldin AL, Escayg A. Altered function of the SCN1A voltage-gated sodium channel leads to gamma-aminobutyric acid-ergic (GABAergic) interneuron abnormalities. The Journal of biological chemistry. 2010; 285:9823–9834. [PubMed: 20100831]

McKinney BC, Chow CY, Meisler MH, Murphy GG. Exaggerated emotional behavior in mice heterozygous null for the sodium channel Scn8a (Nav1.6). Genes Brain Behav. 2008; 7:629–638. [PubMed: 18363861]

Miyoshi H, Blomer U, Takahashi M, Gage FH, Verma IM. Development of a self-inactivating lentivirus vector. J Virol. 1998; 72:8150–8157. [PubMed: 9733856]

Noebels JL. Exploring new gene discoveries in idiopathic generalized epilepsy. Epilepsia 44 Suppl. 2003; 2:16–21.

Norton WT, Poduslo SE. Myelination in rat brain: changes in myelin composition during brain maturation. Journal of neurochemistry. 1973; 21:759–773. [PubMed: 4754856]

Papale LA, Makinson CD, Christopher Ehlen J, Tufik S, Decker MJ, Paul KN, Escayg A. Altered sleep regulation in a mouse model of SCN1A-derived genetic epilepsy with febrile seizures plus (GEFS+). Epilepsia. 2013; 54:625–634. [PubMed: 23311867]

Papale LA, Beyer B, Jones JM, Sharkey LM, Tufik S, Epstein M, Letts VA, Meisler MH, Frankel WN, Escayg A. Heterozygous mutations of the voltage-gated sodium channel SCN8A are associated with spike-wave discharges and absence epilepsy in mice. Hum Mol Genet. 2009; 18:1633–1641. [PubMed: 19254928]

Pfeifer A, Brandon EP, Kootstra N, Gage FH, Verma IM. Delivery of the Cre recombinase by a self-deleting lentiviral vector: efficient gene targeting in vivo. Proceedings of the National Academy of Sciences of the United States of America. 2001; 98:11450–11455. [PubMed: 11553794]

Plummer NW, McBurney MW, Meisler MH. Alternative splicing of the sodium channel SCN8A predicts a truncated two-domain protein in fetal brain and non-neuronal cells. The Journal of biological chemistry. 1997; 272:24008–24015. [PubMed: 9295353]

Raman IM, Sprunger LK, Meisler MH, Bean BP. Altered subthreshold sodium currents and disrupted firing patterns in Purkinje neurons of Scn8a mutant mice. Neuron. 1997; 19:881–891. [PubMed: 9354334]

Royeck M, Horstmann MT, Remy S, Reitze M, Yaari Y, Beck H. Role of axonal NaV1.6 sodium channels in action potential initiation of CA1 pyramidal neurons. Journal of neurophysiology. 2008; 100:2361–2380. [PubMed: 18650312]

Steinlein OK. Genes and mutations in human idiopathic epilepsy. Brain & development. 2004; 26:213–218. [PubMed: 15130686]

Sun W, Wagnon JL, Mahaffey CL, Briese M, Ule J, Frankel WN. Aberrant sodium channel activity in the complex seizure disorder of Celf4 mutant mice. The Journal of physiology. 2013; 591:241–255. [PubMed: 23090952]

Trudeau MM, Dalton JC, Day JW, Ranum LP, Meisler MH. Heterozygosity for a protein truncation mutation of sodium channel SCN8A in a patient with cerebellar atrophy, ataxia, and mental retardation. Journal of medical genetics. 2006; 43:527–530. [PubMed: 16236810]

Veeramah KR, O'Brien JE, Meisler MH, Cheng X, Dib-Hajj SD, Waxman SG, Talwar D, Girirajan S, Eichler EE, Restifo LL, Erickson RP, Hammer MF. De novo pathogenic SCN8A mutation identified by whole-genome sequencing of a family quartet affected by infantile epileptic encephalopathy and SUDEP. Am J Hum Genet. 2012; 90:502–510. [PubMed: 22365152]

Vega AV, Henry DL, Matthews G. Reduced expression of Na(v)1.6 sodium channels and compensation by Na(v)1.2 channels in mice heterozygous for a null mutation in Scn8a. Neurosci Lett. 2008; 442:69–73. [PubMed: 18601978]

Whitaker WR, Faull RL, Waldvogel HJ, Plumpton CJ, Emson PC, Clare JJ. Comparative distribution of voltage-gated sodium channel proteins in human brain. Brain research Molecular brain research. 2001; 88:37–53. [PubMed: 11295230]

Zhou W, Goldin AL. Use-dependent potentiation of the Nav1.6 sodium channel. Biophysical journal. 2004; 87:3862–3872. [PubMed: 15465873]

Highlights

- Hippocampal burst latency and occurrence is reduced in *Scn8a*$^{med/+}$ mice after P20.
- The *Scn8a*-med mutation reduces burst discharges in a GEFS+ model of epilepsy.
- *Cre*-mediated hippocampal knockdown of *Scn8a* confers seizure resistance.
- Global inactivation of *Scn8a* in the adult mouse increases seizure thresholds.
- Selective targeting of *SCN8A* might be efficacious as a treatment for epilepsy.

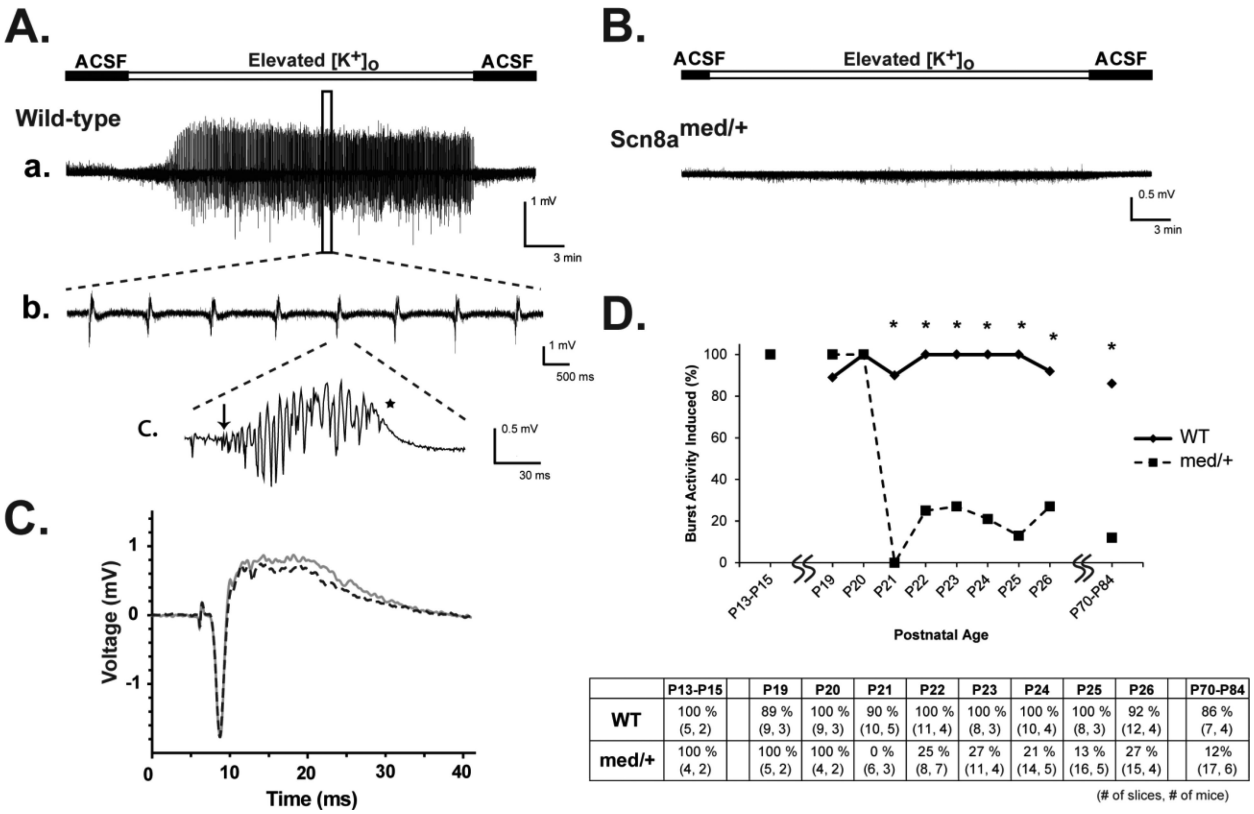

	P13-P15	P19	P20	P21	P22	P23	P24	P25	P26	P70-P84
WT	100 % (5, 2)	89 % (9, 3)	100 % (9, 3)	90 % (10, 5)	100 % (11, 4)	100 % (8, 3)	100 % (10, 4)	100 % (8, 3)	92 % (12, 4)	86 % (7, 4)
med/+	100 % (4, 2)	100 % (5, 2)	100 % (4, 2)	0 % (6, 3)	25 % (8, 7)	27 % (11, 4)	21 % (14, 5)	13 % (16, 5)	27 % (15, 4)	12% (17, 6)

(# of slices, # of mice)

Figure 1.

Spontaneous seizure-like burst discharges in CA3 pyramidal cell layer induced by elevated potassium in hippocampal slices from *Scn8a*$^{med/+}$ mutant and WT mice.

Aa, CA3 pyramidal cells did not show spontaneous burst activity in physiological 2.5 mM $[K^+]_o$; however, burst activity was induced when extracellular K^+ concentration was elevated to 8.5 mM $[K^+]_o$. ***Ab***, Expansion of a segment of spontaneous activity showed synchronous firing of burst activity. ***Ac***, Expansion of a single interictal-like burst discharge. Arrow indicates start of a burst discharge and star shows the end of a single burst. ***B***, Extracellular recording from CA3 pyramidal cell layer of a *Scn8a*$^{med/+}$ mutant mouse (P24). ***C***, Population spike amplitude before and after exposing hippocampal slice to 8.5 mM $[K^+]_o$. Solid gray – before perfusing 8.5 mM $[K^+]_o$ into the bath. Black dash – after exposing slice to 8.5 mM $[K^+]_o$ and washout with standard 2.5 mM $[K^+]_o$ ACSF. Population spikes were evoked with 50 αA stimulation for 100 μs. ***D***, Hippocampal slices from *Scn8a*$^{med/+}$ mutant and WT mice from P13-P20 demonstrated comparable levels of spontaneous burst discharge activity in elevated extracellular potassium. Beginning at P21, the propensity for burst activity dramatically decreased in hippocampal slices from *Scn8a*$^{med/+}$ mutant mice. Number of slices = 4-17, number of mice = 2-7. *$p < 0.001$ when compared to WT; Fisher's exact test with Bonferroni correction.

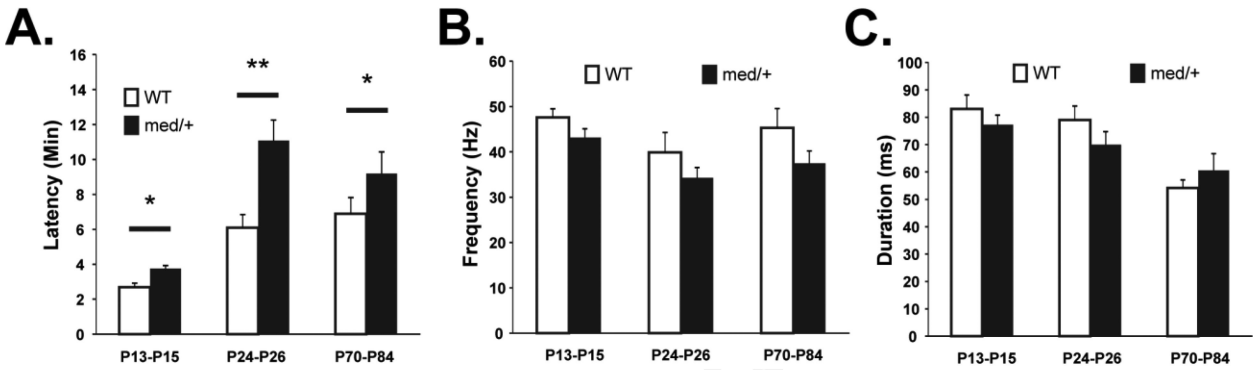

Figure 2.

Analysis of burst characteristics between *Scn8a*$^{med/+}$ and WT mice.

A, Hippocampal slices from *Scn8a*$^{med/+}$ mutants demonstrate longer latencies to the onset of burst activity compared to slices from WT mice for all age groups (WT *vs* mutant at P13-P15: 2.7 ± 0.2 min *vs* 3.8 ± 0.2 min, $p < 0.05$; WT *vs* mutant at P24-P26: 6.1 ± 0.8 min *vs* 11.1 ± 1.2 min, $p < 0.01$; WT *vs* mutant at P70-P84: 6.9 ± 0.9 min *vs* 9.2 ± 1.2 min, $p < 0.05$). Comparison of burst activity showed similar inter-burst frequency ***B***, and burst duration ***C***, between slices from *Scn8a*$^{med/+}$ mutants and WT mice. P13-P15, n = 4-5; P24-P26, n = 6-9; P70-P84, n = 3-5; Student's two-tailed t test, *$p < 0.05$; **$p < 0.001$; error bars indicate SEM.

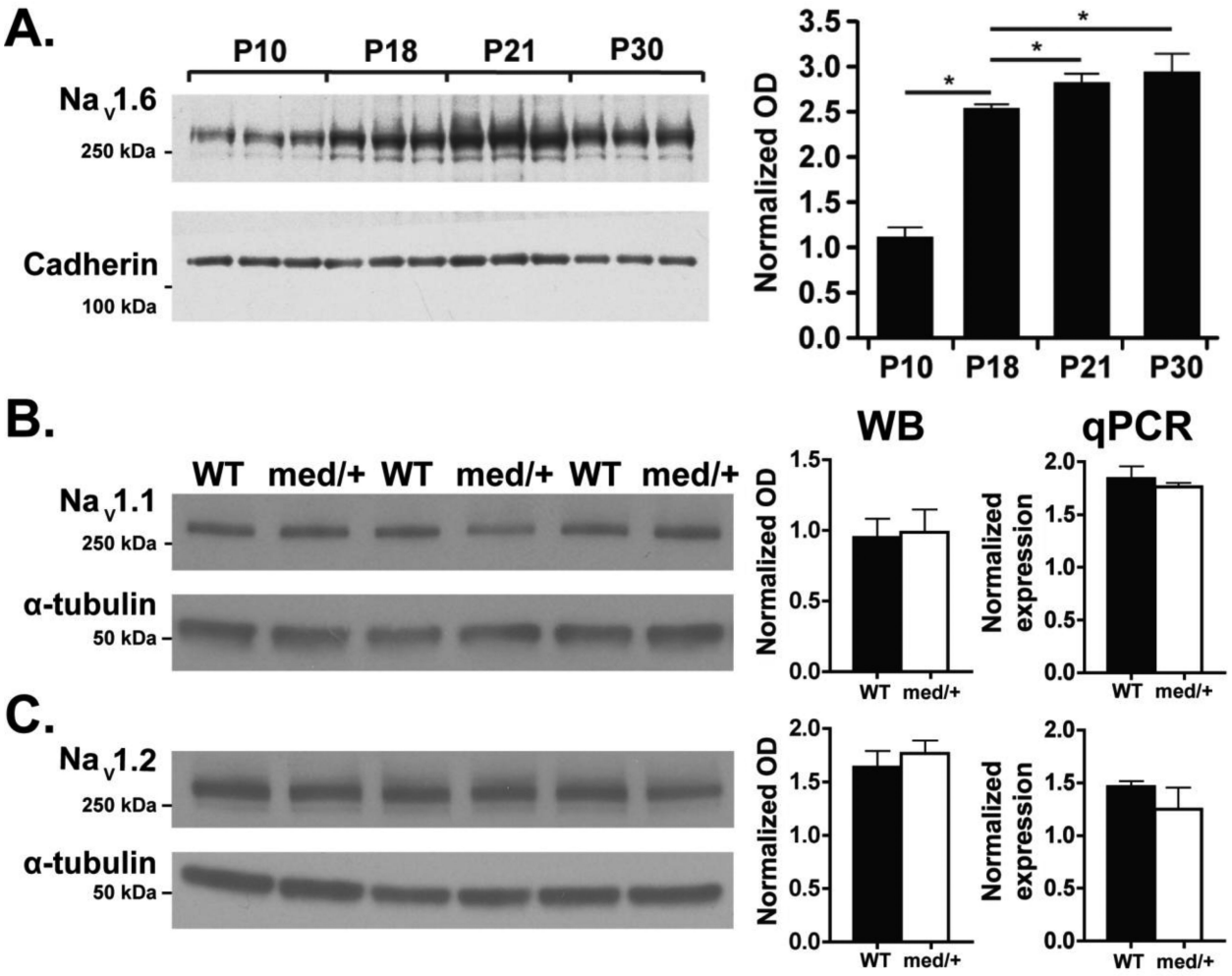

Figure 3.

Developmental expression of VGSCs in the hippocampus of P10-P30 WT mice.

A, Western blot analysis of hippocampal membrane fractions from WT mice using rabbit anti-$Na_v1.6$ polyclonal antibody. Pan-cadherin (135 kDa) was used as a loading control. Statistical analysis of $Na_v1.6$ levels during development was performed using one-way ANOVA; * $p < 0.001$. Post hoc analysis demonstrated that $Na_v1.6$ levels in the hippocampus reach adult levels at 3-4 weeks after birth ($p<0.05$, Holm-Sidak post hoc, n=3 per age group). Hippocampal tissues from WT and *Scn8a*$^{med/+}$ mice were analyzed by Western blotting (WB) and qPCR for alterations in the expression of ***B***, *Scn1a* and ***C***, *Scn2a*. Alpha tubulin (50 kDa) was used a loading control. No significant differences in protein or RNA levels were observed. *Scn1a* and *Scn2a* protein and RNA expression levels were analyzed by the Student's two-tailed t test, $p>0.05$. WB, n = 7 per group; qPCR n = 4-5 per group. Error bars indicate SEM.

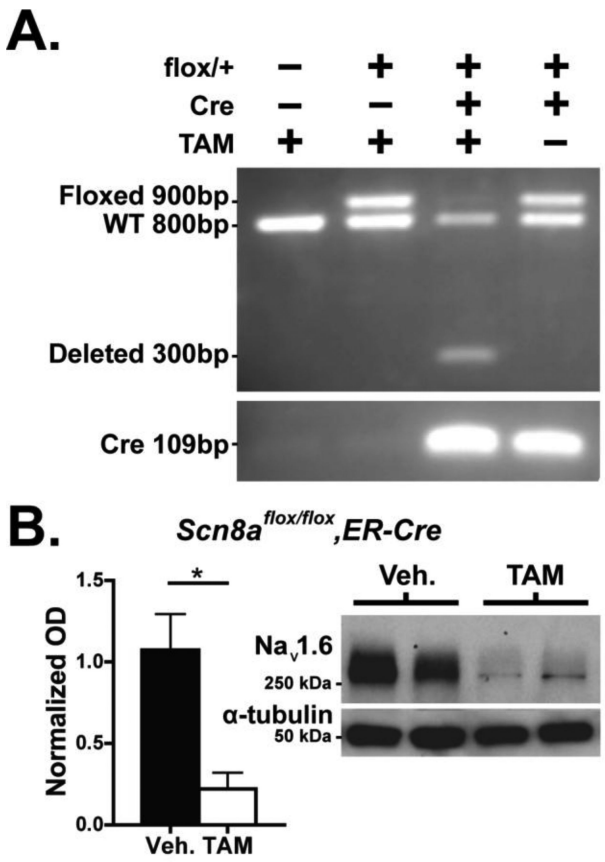

Figure 4.

Tamoxifen-induced global deletion of the *Scn8a* gene.

A, PCR product amplified from dissected neocortical tissue from *flox/+,ER-Cre,*TAM mice as well as control littermates (*flox/+,ER-Cre,*Veh) demonstrated that deletion is only detectable following TAM injection in mice that express the *ER-Cre* transgene and the floxed *Scn8a* allele (third lane). Additionally, the *Scn8a* floxed allele was only marginally detectable following TAM-initiated deletion, providing further evidence of efficient deletion. ***B***, Western blotting demonstrated significant (79%) knockdown of $Na_v1.6$ protein in homozygous floxed mice carrying the *ER-Cre* transgene following TAM injection (*flox/flox,ER-Cre,*TAM) compared to *flox/flox,ER-Cre* mice administered vehicle. n = 3 per group; Student's two-tailed t test, $*p < 0.05$; Error bars indicate SEM. ***C***. Representative Western blot from vehicle and TAM treated *flox/flox,ER-Cre* mice demonstrates reduced band intensity in the TAM treated group.

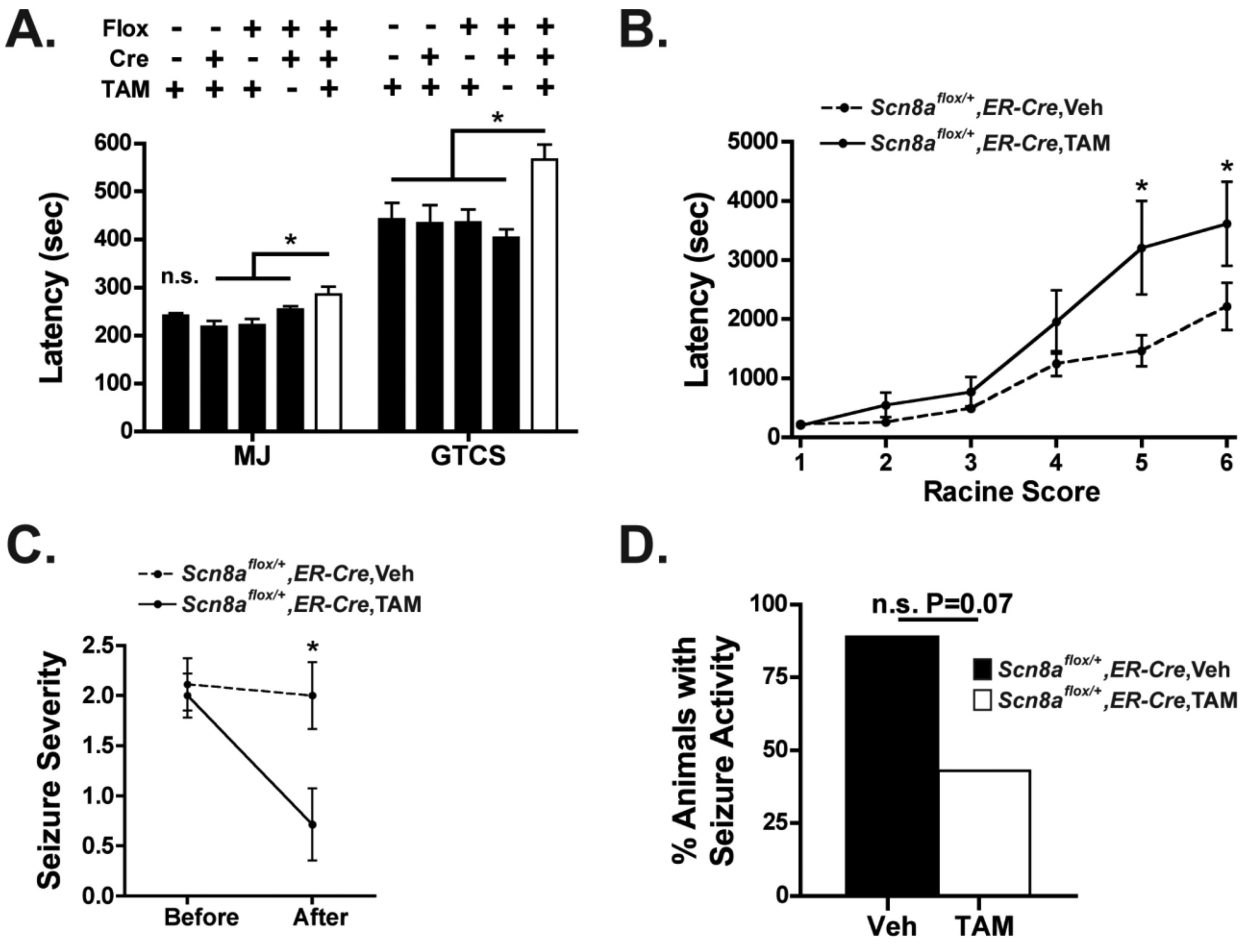

Figure 5.

Inducible deletion of the *Scn8a* gene in the adult mouse is sufficient to increase the latency to flurothyl- and KA-induced seizures and to protect against electrically induced 6-Hz psychomotor seizures.

A, Latencies to flurothyl-induced myoclonic jerk (MJ) and generalized tonic-clonic seizures (GTCS) were increased following TAM-induced inactivation of the *Scn8a* gene (*flox/+*,*ERCre*,TAM) (white bar) compared to control littermates (+/+,no *Cre*,TAM; +/+,ER-*Cre*,TAM; *flox/+*,no *Cre*,TAM; and *flox/+*,*ER-Cre*,Veh) (black bars). n = 10-12 per group. MJ and GTCS, one-way ANOVA, $p < 0.001$; Dunnett's post hoc, $p < 0.05$. ***B***, Latencies to KA-induced seizure events were increased following *Scn8a* deletion (*flox/+*,*ER-Cre*,TAM) (solid line) when compared to vehicle-injected controls (*flox/+*,*ER-Cre*,Veh) (dashed line). Seizure activity was scored using a modified Racine scale: 1 = freezing, 2 = head nodding, 3 = tail clonus, 4 = forelimb clonus, 5 = rearing and falling, 6 = GTCS. n = 12-13 per group. Two-way ANOVA, $p < 0.01$; Bonferroni post hoc, $p < 0.05$. n = 12-13. ***C***, 6-Hz psychomotor seizure severity was decreased after TAM-initiated inactivation of *Scn8a* (*flox/+*,*ER-Cre*,TAM) (solid line) when compared to vehicle-injected controls (*flox/+*,*ER-Cre*,Veh) (dashed line). n = 7-9 per group. Mann-Whitney-U test, $p < 0.05$. Seizure activity was scored using the following modified Racine scale: 1 = freezing, 2 = head nodding 3 = rearing and falling. Average Racine scores: *flox/+*,*ERCre*,Veh. pre = 2.1, post = 2.0; *flox/*

+,*ER-Cre*,TAM pre = 2.0, post = 0.4. ***D***, There was a trend toward reduced 6-Hz psychomotor seizure activity following inactivation of *Scn8a* (*flox/+*,*ERCre*,TAM) when compared to vehicle-injected controls (*flox/+*,*ER-Cre*,Veh). n = 7-9 per group; Fisher's exact test, n.s. $p = 0.07$. *$p < 0.05$; **$p < 0.01$; error bars indicate SEM

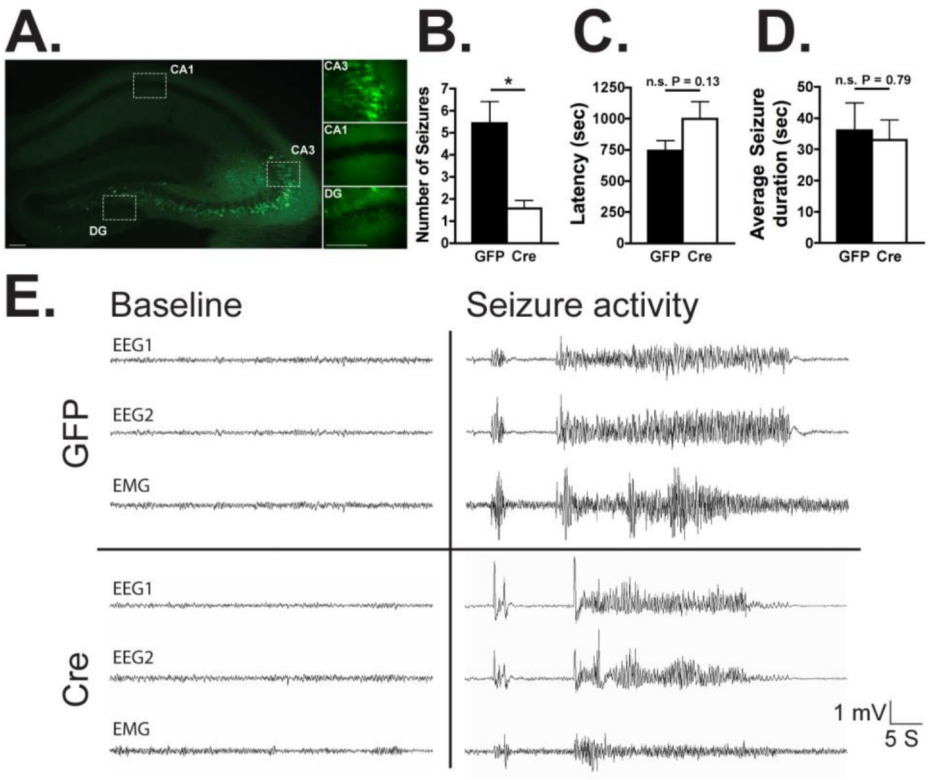

Figure 6.

Lentiviral *Cre*-mediated knockdown of *Scn8a* in the hippocampus reduces seizure activity following PT administration.

Scn8a$^{flox/flox}$ mice were injected with either LV-*GFP* or LV-*Cre* to achieve knockdown of *Scn8a* in the hippocampus. ***A***, *GFP*-positive cells were observed in the CA1, CA3, and DG layers of the hippocampus with highest expression in the DG and CA3. Images were captured at 4X and 40X magnification (inset), scale bar = 100 μm. ***B***, Fewer seizures were recorded in LV-*Cre*- compared to LV-*GFP*-treated mice following PT administration. No significant difference in the latency to the first seizure ***C***, or the average duration of each seizure event ***D***, was observed in LV-*Cre*- compared to LV-*GFP*-injected mice. ***E***, Representative examples of baseline EEG and seizure activity indicating normal baseline EEG activity in both *GFP* and *Cre* groups and seizure activity in *Cre* and *GFP* groups following PT administration. n = 6-7 per group. Mann-Whitney-U test, *$p < 0.05$. Error bars indicate SEM.

Table 1

Genotype	Burst Occurrence (# of slices with bursting/total # of slices)	Burst Latency (min)	Inter-burst Frequency (Hz)
WT	9/9	7.3 ± 0.4 (9)	31.8 ± 2.9 (9)
Scn1a$^{RH/+}$	7/9	4.5 ± 0.3 (7)†	41.9 ± 6.2 (7)
Scn8a$^{med/+}$	2/14*	9.4, 12.7 (2)	20.2, 17.0 (2)
Scn1a$^{RH/+}$; *Scn8a*$^{med/+}$	1/13$^{*\#}$	6.3 (1)	14.3 (1)

Table 2

Summary of main findings

***Scn8a* Genotype**	***Scn1a* Genotype**	**Experimental System**	**Observation**
med/+	+/+	Hippocampal slices with high K^+	Reduced bursting from P21
med/+	*R1648H/+*	Hippocampal slices with high K^+	Decreased bursting in a model of GEFS+
flox/+	+/+	*Scn8a* deletion in adult followed by seizure induction	Increased resistance to flurothyl, kainic acid, and 6Hz-induced seizures
flox/+	+/+	Lentiviral Cre-mediated hippocampal knockdown of *Scn8a* followed by seizure induction	Reduced number of picrotoxin- induced seizures